Experiments with supercooled liquid hydrogen

H. J. Maris, G. M. Seidel, and F. I. B. Williams*
Department of Physics, Brown University, Providence, Rhode Island 02912
(Received 15 April 1987)

We report on experiments performed with droplets of supercooled liquid H_2, maintained in a state of neutral buoyancy in pressurized ^{4}He fluid. We have measured the nucleation rate for solidification as a function of temperature, and have observed and analyzed several interesting hydrodynamic effects relating to the motion of the drops and interactions between them. We discuss the possibility of supercooling liquid H_2 to sufficiently low temperatures to observe the superfluid phase.

I. INTRODUCTION

In this paper we report experiments performed on supercooled liquid hydrogen.[1] This system is of interest because it has been predicted[2] that the amount by which it should be possible to supercool below the normal freezing temperature T_3 should be unusually large. This can be understood as follows. The strength ε_{LJ} of the Lennard-Jones potential between two para-hydrogen (p-H_2) molecules is 37 K. For a classical Lennard-Jones system T_3 is given by

$$kT_3 = 0.7\varepsilon_{LJ} . \quad (1)$$

For p-H_2 this would give $T_3 \sim 26$ K, whereas the actual T_3 is only 13.8 K. The lowering of the freezing temperature is a result of the quantum-mechanical zero-point energy, which is smaller in the liquid phase than in the solid. One can estimate that although the total binding energy of the solid[3] at $T=0$ K is ~ 90 K, the difference in energy between the liquid and solid at $T=0$ K is only ~ 6 K. Thus, the zero-point energy lowers the freezing temperature by almost a factor of 2, and even comes close to making the liquid the stable phase at $T=0$ K. This small difference in energy between the liquid and the solid phases increases the possibility of large supercooling.

In Ref. 2 the rate $\Gamma(T)$ of homogeneous nucleation (per unit volume and time) of the solid phase from the liquid was calculated. This rate is very small, just below T_3, and then increases rapidly with decreasing temperature to a maximum value at around 7 K. Below this temperature the rate falls very rapidly because of the decrease of the thermal energy available to get the system over the nucleation barrier.[4] Thus, if it is possible to cool liquid H_2 through the range of temperatures where Γ is large, one might be able to reach a low-temperature region where the liquid is essentially stable. In this case it would then be possible to reach the superfluidity temperature of liquid H_2, which has been estimated[2] to be 2 or 3 K.

The feasibility of doing an experiment like this depends critically on the maximum value Γ_{max} of the nucleation rate. This quantity depends, in a very sensitive way, on the value of the liquid-solid surface energy α_{LS}. A 10% variation is α_{LS} changes Γ_{max} by more than 10 orders of magnitude. A measurement of Γ at any temperature, however, enables one to determine α_{LS} by comparison with the theory.[5] The theory can then be used to predict Γ at other temperatures, specifically, an estimate could be made of Γ_{max}.

In this paper we report on measurements of $\Gamma(T)$ in the temperature range 10.6–11.2 K, and we use this data to calculate α_{LS}. We also describe several interesting hydrodynamic effects which have been observed in these experiments. Finally, we will discuss the prospects for the production of superfluid H_2.

II. EXPERIMENT

To study the homogeneous nucleation rate it is necessary to eliminate heterogeneous nucleation. Thus, the liquid must be free of impurities and should not be in contact with the solid walls of a container, etc. To eliminate a container one could study liquid drops in free fall, do an experiment in a zero-gravity environment, or study a cloud of fine droplets falling very slowly through helium gas. Another possibility is to levitate the sample acoustically[6] or by means of electromagnetic radiation.[7] In our experiment we have levitated liquid-H_2 drops by making them neutrally buoyant in ^{4}He fluid. The critical temperature T_c of ^{4}He is 5.2 K, so that above this temperature it is possible to vary the density of ^{4}He fluid continuously over a wide range. At any temperature above T_c there exists a certain pressure at which liquid H_2 and fluid ^{4}He will have the same density. We calculate this pressure in the Appendix, and show the result over the range of temperature 10–12 K in Table I.

The design of our experiment is shown in Fig. 1. For most of the measurements of nucleation rate the cell was a cylindrical chamber 5 cm in diameter and 6.5 cm long. In some of the earlier experiments a cell only 1.3 cm long was used. The walls of the cell are 0.5-cm-thick Pyrex glass and are indium-sealed to thick copper end plates. The cell is held together by six 0.12-cm-diam stainless-steel bolts which run vertically between the two end plates. The cell is cooled by a post (copper with a stainless-steel section), the upper end of which is at-

TABLE I. Pressure at which liquid H_2 floats in helium fluid as a function of temperature.

T (K)	P (bars)	T (K)	P (bars)
10	13.03	11	15.31
10.2	13.49	11.2	15.76
10.4	13.95	11.4	16.21
10.6	14.40	11.6	16.66
10.8	14.86	11.8	17.11

tached to the lower plate and the lower end immersed in the main liquid-^{4}He bath. The temperatures of the end plates are controlled by heaters, and in a typical case these temperatures are 15 K for the top plate and 7 K for the bottom. Because of this temperature gradient, the ^{4}He density in the cell decreases with height. The copper end plates serve to reduce horizontal temperature gradients, and any resulting convection currents. There is some height at which the density of the ^{4}He matches that of liquid H_2 (the "liquid level"), and at a lower height solid H_2 will be neutrally buoyant ("solid level").

The cell is prepared for an experiment by pumping on it at room temperature for several days and flushing it with ^{4}He gas. It is then cooled to low temperatures while under vacuum. ^{4}He is introduced into the cell through a filter which is immersed in the main ^{4}He bath. This filter was made of 1-μm alumina powder sandwiched between sintered copper powder. The cell was filled to the desired pressure (13–17 bars) in about 1 h. The H_2 drops were formed by introducing liquid H_2 into the cell through an orifice of 10 μm diam cut in a stainless-steel disk of 25 μm thickness mounted in the center of the top plate. This liquid H_2 had been converted to p-H_2 by passing it through 5 cm^3 of nickel silicate at 15 K in an external Dewar. Before entering the cell it passed through a filter, similar to the ^{4}He filter, which was at 20 K. The starting H_2 was 99.995% pure,[8] not counting the 0.015 at. % of deuterium as an impurity.

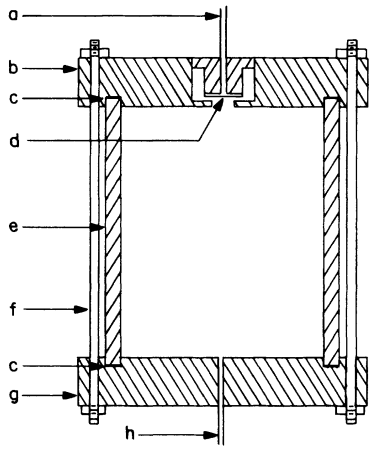

FIG. 1. Experimental cell. (a) H_2 fill line. (b) Top copper end plate. (c) Indium seal. (d) Stainless-steel plate with orifice. (e) Pyrex cylinder. (f) Stainless-steel bolt (one of six) holding cell together. (g) Bottom copper end plate. (h) ^{4}He fill line.

Once the cell was filled with ^{4}He and the upper fill line containing H_2 liquid, the system was left for $\sim$30 min so that thermal equilibrium was established. The pressure on the H_2 was then raised by $\sim$0.5 bar for 10–30 sec, and then returned to its original value. This produced a jet of liquid H_2 which broke into fine droplets. As the droplets slowed because of interaction with the helium fluid, coalescence occurred.[9] When the overpressure on the H_2 was small, the jet velocity was low and large drops (100–500 μm diam) were obtained. For larger overpressure the drop size decreased, and some drops were produced whose diameter was in the range below 40 μm.

The droplets were observed through a long-working-distance microscope.[10] Because we viewed the drops through the cylindrical cell wall and the four layers of curved glass of the Dewar,[11] it was impossible to measure the sizes of drops whose diameter was below $\sim$30 μm. A video camera attached to the microscope and video recorder were used to record the motion of the drops and nucleation events.

III. RESULTS

Liquid-H_2 drops were introduced into the cell, and settled at the liquid level. There was, on occasion, a small horizontal drift of the drops which must have originated from convection currents in the cell produced by the disturbance of the jet. Occasionally drops were seen to collide and coalesce, as we will describe later. In general, however, the drops were remarkably stable and individual drops could be observed (depending on temperature) for as long as 30 min.

A. Jumping drops

When the pressure in the cell is slowly lowered, the liquid drops move to a new level to satisfy the buoyancy condition, and their temperature is lowered. For large drops (diameter 500–1000 μm) one begins to see nucleation of the solid at $\sim$16 bars. When nucleation occurs the drops do not simply fall to the solid buoyancy level. Instead, they first jump upwards and then fall. The reason for this is as follows. When nucleation occurs the latent heat of fusion is liberated, and the drop warms. The hot drop heats a layer of the surrounding helium fluid, and this layer expands and moves upward dragging the hydrogen drop with it (Fig. 2). Eventually the heat stored in the hydrogen drop is exhausted, and the drop then falls rapidly to the solid level.

In Fig. 3 we show measurements of the height z of several drops as a function of the time t after the solid has nucleated. These data were obtained by measuring the position of a drop on individual frames of a video recording.[12] The time between frames was $\frac{1}{30}$ sec. At first sight the data appear to be well described by a parabola, i.e., the drop appears to have an initial upward velocity and a subsequent motion described by a constant downward acceleration g^*. For this to happen the drop would have to cool very rapidly (in 0.1 sec, or less), which would give an upward force due to the helium

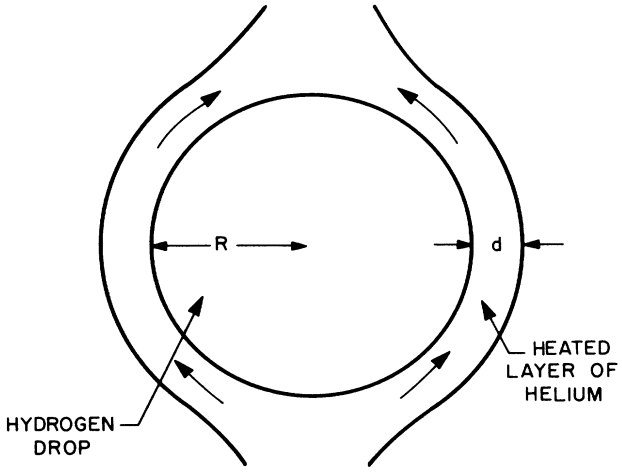

FIG. 2. Schematic diagram of the heated layer of helium flowing around the drop.

lasting only for a short time. One would also need the drag exerted on the drop by the helium during the remainder of the trajectory to cause insignificant effects. It is easy to show that this interpretation is incorrect. For the drops shown in Fig. 3, the values of g^* required to fit the data vary from drop to drop and are less than 10 cm sec^{-2}. This compares with the expected value of

$$g^* = \frac{\rho_S - \rho_L}{\rho_S + \frac{1}{2}\rho_G} g \cong 70 \text{ cm sec}^{-2} , \tag{2}$$

where ρ_S and ρ_L are the densities of solid and liquid hydrogen, ρ_G is the density of the gas, and the effect of the backflow around the solid sphere has been included through the $\frac{1}{2}\rho_G$ term in the denominator.

To try to obtain a satisfactory understanding of the data, we calculate the terminal velocity of solid drops. For the viscous force exerted by the helium we use the expression[13]

$$F = 6\pi\eta_G v R \{1 + 0.15[N(\text{Re})]^{0.687}\} , \tag{3}$$

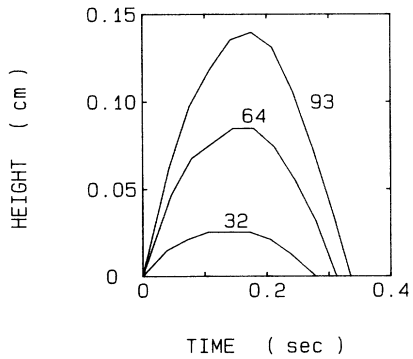

FIG. 3. Height z of a drop as a function of the time t after the nucleation of the solid. The heights were measured at intervals of $\frac{1}{30}$ sec from a video tape recording. Results for different drops are labeled by the drop radius in μm.

where R is the radius of the drop, v the velocity, η_G the viscosity of the helium fluid, and the Reynolds number is

$$N(\text{Re}) = \frac{2Rv\rho_G}{\eta_G} . \tag{4}$$

The terminal velocity v_∞ is then the solution of the equation

$$v_\infty = \frac{2}{9}\frac{R}{\eta_G}(\rho_S - \rho_L)g / \{1 + 0.15[N(\text{Re})]^{0.687}\} , \tag{5}$$

This assumes the drop has completely solidified and is at the temperature of the helium. Terminal velocities calculated from (5) are in excellent agreement ($\pm 10\%$) with the velocity of the drops as they return to height zero. We have checked this for drops with R between 30 and 200 μm. These data thus imply that on the downward part of the trajectory the drop is solid.

The time to reach the terminal velocity is quite short. For $R = 100$ μm, for example, v_∞ / g is only 0.02 sec, i.e., less than one frame of the recording system. This result implies that in the earlier part of the trajectory the *inertia* of the drop can probably be ignored, i.e., the velocity of the drop is determined by a balance between the instantaneous values of the viscous drag force F_v exerted on the drop by the convecting helium, and the gravitational force F_g due to the increased density of the hydrogen as it becomes solid. The variation of the velocity with time is due to the change of these two forces as the drop cools.

Consider first how the temperature of the drop changes after nucleation occurs. Let the temperature of the drop before freezing be T_0, and let the enthalpies per mole of liquid and solid at temperature T be $h_L(T)$ and $h_S(T)$. In the time before any heat leaves the drop the enthalpy will remain constant. However, the enthalpy of the liquid for T_0 in the range of interest (10.6–11.2 K) is greater than h_S at T_3. Hence, after nucleation the drop must be a mixture of liquid and solid at temperature T_3. The fraction of the mass of the drop which is solid is therefore

$$f = \frac{h_L(T_3) - h_L(T_0)}{h_L(T_3) - h_S(T_3)} . \tag{6}$$

For T_0 at 11 K this fraction is ~ 0.3. The fractional change in volume of the drop is then

$$\frac{\delta V}{V} = f\left[\frac{\rho_L(T_0)}{\rho_S(T_3)} - 1\right] + (1-f)\left[\frac{\rho_L(T_0)}{\rho_L(T_3)} - 1\right] . \tag{7}$$

It turns out that the decrease in density due to the thermal expansion of the part remaining liquid very nearly cancels the increase in density of the part of the drop that freezes. In the range $11.5 \geq T_0 \geq 10.5$ K, $|\delta V/V|$ is always less than 0.002, whereas when the drop has completely frozen $\delta V/V = -0.09$. Thus, F_g is initially essentially zero and only becomes appreciable as the drop cools.

To estimate the rate at which the drop cools we have to consider both heat loss from the surface of the drop and heat transport within the drop. For the rate $\dot{Q}$ at which the drop loses energy to the helium we use[14]

$$\dot{Q}=4\pi R\,\Delta T\kappa_G\{1+0.557[N(\mathrm{Gr})]^{1/4}[N(\mathrm{Pr})]^{1/4}\}\ , \tag{8}$$

$$N(\mathrm{Gr})=\frac{\rho_G^2 g\beta_G\Delta T R^3}{\eta_G^2}\ , \tag{9}$$

ρ_G, β_G, and η_G are the density, expansion coefficient, and viscosity of the helium, and ΔT is the excess temperature of the surface of the hydrogen relative to the helium. $N(\mathrm{Pr})$ is the Prandtl number $(C_p\eta_G/\rho_G\kappa_G)$, where C_p is the specific heat per unit volume of the helium, and κ_G is the thermal conductivity. Equation (8) is an approximate result for a solid sphere held at rest in a large volume of gas. For the drop to freeze, but still be at T_3, we have to remove an amount of heat

$$\Delta Q=\frac{4}{3}\frac{\pi R^3}{v_L(T_3)}[h_L(T_3)-h_S(T_3)]\ , \tag{10}$$

where v_L is the molar volume of the liquid. As heat is lost by the drop a solid layer will form at the surface. If the conductivity of the solid is high enough the temperature at the surface of the drop will stay at T_3 until the entire drop has frozen. Thus, ΔT will be equal to T_3-T_0. Given this assumption, one can calculate from (8) and (10) the time τ_F for the drop to freeze. This time comes out to be 0.005 sec for $R=32$ μm and 0.023 sec for $R=93$ μm. These times are both short compared to the time τ_{up} the drops take to reach the maximum height. A possible reason for this, at least for the larger drops, can be understood from Eq. (8). The second term, which involves the Grashof number, represents the contribution to the cooling rate due to convection of the helium *relative* to a drop, which is held fixed. In our experiment the drop is free to move and, particularly in the early stage when its density is close to that of the helium, will have a velocity close to that of the helium. Thus, Eq. (8) overestimates the cooling rate, especially for large drops where the convection term in Eq. (8) is much larger than the conduction term. For example, if we drop the convection term the freezing times τ_F become 0.01 and 0.12 sec for the 32- and 93-μm drops. For the 93-μm drops this would then be sufficiently long to explain the observed τ_{up}.

Consider now the heat transport within the drop. Suppose that the cooling at the surface is perfect, i.e., the surface is held by the helium gas at T_0. Then one can show that the time for the drop to become completely frozen is[15]

$$\tau_F'=f\frac{l_{\mathrm{LS}}R^2}{6\kappa_S\Delta T}\ , \tag{11}$$

where l_{LS} is the latent heat per unit volume, and κ_S is the thermal conductivity of the solid. If we use measured values[3] of κ_S ($\sim 10^5$ cgs at 12 K), we find τ_F' equal to 0.001 sec for $R=32$ μm and 0.008 sec for 93 μm. These times are much less than the time for heat to leave the drop, and this would imply that the assumption of negligible temperature gradients in the solid layer is reasonable. It is possible that since the hydrogen has frozen quickly, it has a conductivity much lower than that for ordinary crystals. However, it seems unlikely that this could be a big enough effect to make τ_F' as large as τ_{up} for the 32-μm drop.

Finally, consider the upward force on the drop due to the convection. For simplicity, we make an approximate calculation[16] of the force when the velocity of the drop is zero; the extension to a moving drop is straightforward. Let the thickness of the layer of helium which is heated be d (see Fig. 2), and let its velocity be v_l. We assume that $d\ll R$ and that the whole helium layer has excess temperature ΔT. The thickness of the layer must be related to the time t for the layer to flow round the drop by

$$d=(\kappa_G t/C_p)^{1/2}\ . \tag{12}$$

The time is related to the velocity by

$$t=\frac{\pi R}{v_l}\ . \tag{13}$$

For steady-state flow the viscous drag on the moving layer must balance the buoyancy force. Thus,[17]

$$4\pi R^2 d\rho g\beta_G\Delta T=16\pi R^2\eta_G v_l/d\ . \tag{14}$$

The upward drag force F_d exerted by the convecting layer is then half the buoyancy force on the layer, and this can be expressed as

$$F_d=\frac{2^{3/2}\pi^{5/4}[N(\mathrm{Gr})]^{3/4}}{[N(\mathrm{Pr})]^{1/4}\rho_G}\eta_G^2\ . \tag{15}$$

As a reference point, we can compare this force with the gravitational force on the drop when it is completely solid, which is

$$\tfrac{4}{3}\pi R^3(\rho_S-\rho_L)g\ . \tag{16}$$

F_d is bigger than this if

$$\Delta T>150R\ , \tag{17}$$

where R is in cm. Thus, the drag force is certainly large enough to make drops of the size we have measured more upward initially.[18] We have, in fact, observed that very large drops ($R>500$ μm) scarcely jump at all, and this is qualitatively consistent with Eq. (17).

The calculation just given assumes in several places that $R\gg d$. Numerically Eqs. (12)–(14) give

$$d=\frac{0.01R^{1/4}}{\Delta T^{1/4}}\ . \tag{18}$$

Thus, for $\Delta T=3$ K d is 24 μm for $R=93$ μm. However, if $R=32$ μm, d is 18 μm and the layer is no longer thin compared to the radius. For very small drops a different picture is more appropriate. In a very short time heat will diffuse from the drop into a volume of gas which is larger than the drop size. This heated sphere of gas will then convect upwards, and will drag the small hydrogen drop with it. Eventually, the drop will fall out of the region of heated gas, and will then descend. We have not studied this process in detail, but it may be able to explain why the small drops take longer to reach their maximum height than one would expect based on the calculated cooling time.

B. Height variations

When the liquid drops are observed carefully one finds that there is an appreciable variation in the heights at which they float. We considered several possible explanations of this effect. Since the liquid drops are in a vertical temperature gradient there will be a small force due to thermophoresis.[19] This force is proportional to the radius R of the drop and, since the buoyancy force varies as R^3, will cause different drops to float at different heights. However, this effect is too small and is in the wrong direction. There is a diffusiophoresis force arising from the gradient in the density of H_2 in the He fluid. This also is too small. An axially symmetric convection current in the cell would give a vertical force proportional to R, and would therefore cause different size drops to float at different heights. It is likely that small currents of this type do exist in the cell.[20] However, they should cause a height variation which is larger near the axis of the cell than near the walls, and this is not observed.[21]

A significant clue to the origin of the effect is the observation that there is no such effect for the drops after they have frozen and are at the solid level. A force which exists on a liquid drop, but not a solid drop, arises from the temperature dependence of the liquid-gas surface tension α of the liquid drop. The bottom of the liquid drop is colder than the top, and hence has a larger surface tension. This produces a tangential force on the surface of the drop, and the surface also flows from the top to the bottom (Fig. 4). There is therefore a flow induced in the helium and inside the drop. In the steady state the viscous forces due to these induced flows balance the force on the surface resulting from the gradient in the surface tension. If we assume that the flow velocity $\mathbf{v}$ is small, we have to solve the linearized Navier-Stokes equations

$$\eta\nabla^2\mathbf{v}=\text{grad}P\ , \tag{19}$$

$$\text{div}\mathbf{v}=0\ . \tag{20}$$

In addition, $\mathbf{v}$ must vanish at infinity, be continuous, and have zero derivative normal to the surface of the sphere. We have temporarily ignored the effect of gravity. For the tangential forces on the surface of the sphere to balance we need

$$\sin\theta\frac{\partial\alpha}{\partial z}=\sigma'_{r\theta,G}-\sigma'_{r\theta,L}\ , \tag{21}$$

where $\sigma'_{r\theta,G}$ and $\sigma'_{r\theta,L}$ are the viscous tangential stresses at the surface of the drop in the gas and liquid, respectively. Let the temperature gradient in the vertical direction in the cell far away from the drop be T'. Then, since the flow is assumed to be small,[23] the temperature gradient inside the drop will be

$$\frac{\partial T}{\partial z}=\frac{3\kappa_G}{\kappa_L+2\kappa_G}T'\ , \tag{22}$$

and so

$$\frac{\partial\alpha}{\partial z}=\frac{3\kappa_G}{\kappa_L+2\kappa_G}T'\frac{d\alpha}{dT}\ . \tag{23}$$

Since α varies over the surface of the drop, the drop must become nonspherical in order for the normal forces to balance. This is a very small effect, since the significant parameter is

$$\frac{R}{\alpha}\frac{\partial\alpha}{\partial z}\ll 1\ . \tag{24}$$

One can solve Eqs. (19)–(21) for a sphere which is held at rest by applied body forces.[23] Outside the sphere the solution is

$$v_r=2u_0\left[\frac{R^3}{r^3}-\frac{R}{r}\right]\cos\theta\ , \tag{25}$$

$$v_\theta=u_0\left[\frac{R}{r}+\frac{R^3}{r^3}\right]\sin\theta\ , \tag{26}$$

$$P=P_0-\frac{2\eta_G u_0 R\cos\theta}{r^2}\ . \tag{27}$$

Within the sphere

$$v_r=2u_0\left[1-\frac{r^2}{R^2}\right]\cos\theta\ , \tag{28}$$

$$v_\theta=2u_0\left[-1+\frac{2r^2}{R^2}\right]\sin\theta\ , \tag{29}$$

$$P=P_0-\frac{20\eta_L u_0 r\cos\theta}{R^2}\ , \tag{30}$$

with

$$u_0=-\frac{1}{6}\frac{\partial\alpha}{\partial z}\frac{R}{\eta_L+\eta_G}\frac{3\kappa_G}{\kappa_L+2\kappa_G}\ , \tag{31}$$

and P_0 is equal to the pressure at the center of the drop. The flow pattern is shown in Fig. 4. Given the flow velocity, it is straightforward to show that there is a

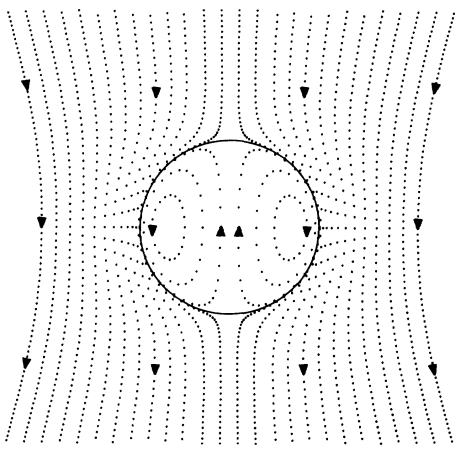

FIG. 4. Flows of hydrogen and helium induced by the variation of the surface tension. The figure shows steamlines, and the spacing between the dots indicates the velocity.

viscous force F_α upwards on the sphere

$$F_\alpha = -4\pi \frac{\eta_G R^2}{\eta_L + \eta_G} \frac{\kappa_G}{\kappa_L + 2\kappa_G} \frac{d\alpha}{dT} T' \ . \tag{32}$$

This is positive because $d\alpha/dT$ is negative. The drop will be pushed up until it reaches a height h at which the buoyancy force F_B balances F_α. Now

$$F_B = \tfrac{4}{3}\pi R^3 \left[\frac{\partial \rho_G}{\partial T} \right]_P g T' h \ . \tag{33}$$

Hence, the displacement of the drop from the level at which $\rho_L = \rho_G$ is

$$h = \frac{A}{R} \ , \tag{34}$$

with

$$A = \frac{1}{g} \frac{\eta_G}{\eta_L + \eta_G} \frac{3\kappa_G}{\kappa_L + 2\kappa_G} \left| \frac{d\alpha}{dT} \right| \left[\frac{\partial \rho_G}{\partial T} \right]_P^{-1} \ . \tag{35}$$

As shown in Fig. 5, the height as a function of R is fairly well described by the R^{-1} law predicted by Eq. (34). We have tested this at several temperatures, and used the data to find values for A (Table II). To calculate A we have had to estimate the parameters for the supercooled liquid. We used

$$\eta_L = 1.06 \times 10^{-4} e^{15.78/T} \ , \tag{36}$$

$$\kappa_L = 668 + 566T \ , \tag{37}$$

and

$$\frac{d\alpha}{dT} = -0.016T \ . \tag{38}$$

These values (all in cgs units) are extrapolated from the region where measurements exist above 14 K. The theoretical values of A are shown in Table II, and are 2–3 times larger than the experimental results. There are several possible reasons for this: (1) Equation (38) is obtained from the measured surface tension of liquid H_2 at saturated vapor pressure. We have measured the effect of high-pressure helium gas on α, and found a reduction of α of 30–40 % in the pressure range 10–20 bars. (2) The viscosity η_L may increase with decreasing T more rapidly than Eq. (36) predicts. (3) The assumption of a small velocity flow is not valid under the conditions of our experiment. If the flow is too large the temperature gradient in the vicinity of the drop is altered by the convection, and the force on the drop will be changed. The magnitude of the corrections arising from the alteration of the temperature gradient by the flow are measured by the Marangoni number,[24] and for the conditions of our experiment there should be a significant change in the force. In addition, if the velocity is large one cannot use the linearized Navier-Stokes equation (19), and the term $\rho(\mathbf{v}\cdot\nabla)\mathbf{v}$ must be added. The relative importance of this term can be characterized by a Reynolds number $N(\mathrm{Re})$, defined as

$$N(\mathrm{Re}) = \frac{2Rv_e\rho_G}{\eta_G} \ , \tag{39}$$

where v_e is the velocity at the equator of the drop $(-2u_0)$. At 11 K, for example, we find that when the temperature gradient is 1 K cm^{-1},

$$N(\mathrm{Re}) = 2.7 \times 10^5 R^2 \ . \tag{40}$$

Thus, for a 100-μm-radius drop $N(\mathrm{Re})$ is 27, and there must be significant corrections to the linearized Navier-Stokes equation.

TABLE II. Experimental and theoretical results for the parameter A in Eq. (34).

T (K)	A^{expt} (cm^2)	A^{theor} (cm^2)
10.6	1.9×10^{-4}	5.5×10^{-4}
11.1	2.5×10^{-4}	6.7×10^{-4}
11.2	3.0×10^{-4}	7.0×10^{-4}
12	3.5×10^{-4}	9.4×10^{-4}

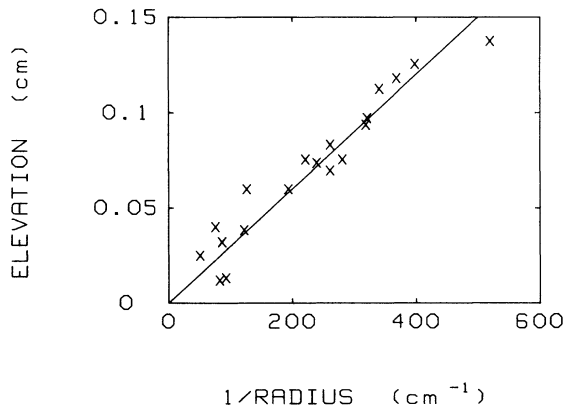

FIG. 5. Elevation of the drops plotted versus the inverse of the radius R at 11.2 K. The straight line is a fit to the data using $h = A/R$, with $A = 3.0\times10^{-4}$ cm^2.

C. Forces between drops

There are several interesting effects (Fig. 6) which occur when two drops are near each other, i.e., within a few diameters. Two drops of equal size will float at the same height. If they are sufficiently close together in the horizontal plane, they accelerate towards each other and collide, Fig. 6(a). A second effect occurs when a large drop drifts into a position underneath a small drop which is floating at a higher level because of the effects just discussed. The large drop pulls the small drop down towards it. However, instead of a collision occurring, the small drop settles into a stable configuration a distance smaller than the diameter of the small drop above the top of the big drop, Fig. 6(b). This "drop-on-drop" effect (DOD) sometimes produces vertical columns of as many as four drops Fig. 6(c), the largest at the bottom and the smallest at the top.

Both of these effects must be caused by the velocity field discussed in the preceding section. The DOD effect

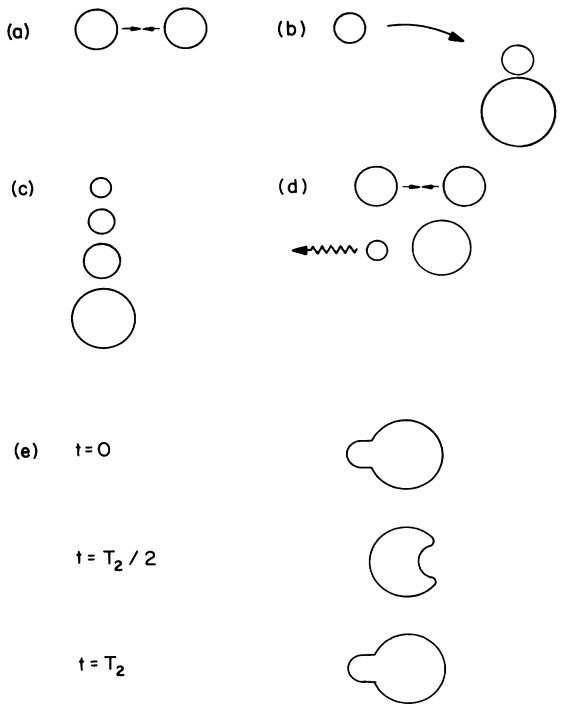

FIG. 6. Interactions between drops. (a) Two drops of roughly equal size floating at same height are attracted to each other. (b) A small drop is pulled down by a big drop and settles into a stable position above it. (c) A column of drops is formed. (d) Collision of two drops of roughly the same size. A small drop is ejected at high velocity (wavy arrow) in the direction shown. (e) Possible shape of the drop after the collision. For discussion see text.

is only seen in the short cell where the temperature gradient is typically 8 K cm^{-1}. In this case the Reynolds number is large, and so the flow pattern induced by the surface tension force will be substantially different from the result we have calculated in the linear approximation. Thus, it is impossible to give a quantitative discussion of the forces between drops. It is clear that a large drop will produce a downward flow of the helium gas above it, and that this flow can pull a small drop down from the higher level it would otherwise occupy as a result of its own flow pattern, Eq. (34). However, it is hard to understand why the small drop ends up in a configuration of stable equilibrium. For example, suppose the small drop is in equilibrium under the influence of the buoyancy force, its internally generated surface-tension levitating force, and the Stokes drag force due to the flow generated by the big drop, as given by Eqs. (25) and (26). It is easy to show that for the small drop to have lateral stability under the influence of these forces its height above the center of the big drop (radius R_B) must be at least $R_B\sqrt{3}$. Experimentally the drops are seen to be considerably closer together than this. This could be because the flow pattern of the big drop is changed due to the large value of $N(\mathrm{Re})$.

Calculations of the interactions between two bubbles in a liquid have been performed by Meyyappan and Subramanian,[25] and some experimental observations have also been made.[26] These calculations are for bubbles moving under the influence of forces of surface tension only (no gravity), and it is assumed that the flow velocity is small. Consequently we cannot compare our observations and these calculations.

D. Collisions between drops

As mentioned above, two drops of roughly equal size floating at the same height experience an attractive force if they are close to each other. After collision, instead of forming a single large drop, a small drop is usually ejected as shown in Fig. 6(d). This small drop always appears on the side of the coalesced drop where the smaller of the two original drops was originally (the "front" of the drop). In a typical case the radius of the ejected drop is $\sim\frac{1}{4}$ of the radius of the coalesced drop. One cannot resolve the ejection process with the video recorder. In one frame the drops have not collided, and in the next the collision has occurred, the small drop having already moved, typically, 1 mm away. Thus, the ejection velocity must be at least 3 cm sec^{-1}.

We have not been able to find this effect described in the literature, although many experiments have been performed to study the coalescence of water drops. Most studies of water have been performed to understand the distribution of drop sizes in rain. In general, the results of these experiments show that at low relative velocities single coalescence occurs.[27] Park[28] has reported an effect called "reflex disjection" in which there is an ejected drop moving in the same direction as we observe (i.e., leaving from the front of the drop) but apparently in his experiments (with water in nitrogen gas) this effect is *not* seen when the initial relative velocity of the starting drops is very small. In general, the rain-drop studies are mostly concerned with much larger approach velocities than in our experiment.[29]

The kinetic energy of the ejected drop clearly comes from the change in the surface energy of the system. If drops of radii R_1 and R_2 collide to produce a single big drop, the surface energy decreases by

$$\Delta E = 4\pi\alpha[R_1^2+R_2^2-(R_1^3+R_2^3)^{2/3}] . \tag{41}$$

If all this were converted into the kinetic energy of a small ejected drop of radius R' ($R' \ll R_1, R_2$), the velocity of ejection would be v given by

$$v^2 = \frac{6\alpha[R_1^2+R_2^2-(R_1^3+R_2^3)^{2/3}]}{\rho_L R'^3} . \tag{42}$$

For $R_1 = 100$ μm, $R_2 = 150$ μm, $R' = 30$ μm, and $\alpha = 3$ cgs, we find $v = 5.7$ cm sec^{-1}, of the same general magnitude as is observed.

We think that the kinetics of the effect may possibly be understood in terms of the modes of oscillation of the drop. For a liquid drop in a gas of the same density the normal-mode frequencies ω_n are given by[30]

$$\omega_n = A_n(\alpha/\rho_L R^3)^{1/2} , \tag{43}$$

$$A_n = [(n-1)n(n+1)(n+2)/(2n+1)]^{1/2} . \tag{44}$$

The lowest mode has $n=2$ and, for a 100 μm radius drop, has period $T_2=0.47$ msec. The damping of the mode comes principally from the viscosity of the liquid; the time τ_n for the amplitude of the nth mode to attenuate is[30]

$$\tau_n=\frac{1}{n^2-1}\rho_L\frac{R^2}{\eta_L} . \tag{45}$$

The lowest modes are lightly damped; we find, for example, that for $n=2$ the quality factor at 11 K is 40. Consequently, it is possible that when the drops coalesce, several modes of the drop are excited, and that at a later time these modes interfere constructively at some point on the surface with such a large amplitude that a small drop is ejected. Equivalently, one can describe the process in terms of a wave propagating around the drop. From the wave picture it would seem at first sight that the large amplitude might appear at the back of the drop. This is because the cylindrically symmetric waves, which are generated at the front when coalescence occurs, will first come back together when they reach the back. However, this argument ignores the peculiarities of the dispersion of surface waves on a drop, or equivalently the harmonic relations between the mode frequencies. The A_n coefficients for $n=2$–6 have the values 2.191, 4.140, 6.325, 8.739, and 11.368. Thus, the modes are very close to being harmonically related, but ω_n is proportional to $n-1$, instead of n. It is easy to show that the modes interfere constructively at the back of the drop after a time of $\frac{1}{2}T_2$, but that the displacement of the surface is inward [Fig. 6(e)] and so there is no tendency for a small drop to be ejected. At $t=T_2$ each of the low-n modes has gone through approximately a whole number of cycles, and so the shape of the drop is close to what it was at $t=0$, i.e., there is a bump outwards at the front [Fig. 6(e)]. This description assumes that the oscillations of the drop are small, whereas in fact they are large and so there will be significant nonlinear effects. We have to assume that these nonlinearities are such that the bump reappearing at the front at T_2 becomes sharpened sufficiently to cause a small drop to be ejected.

E. Nucleation rate measurements

To measure the nucleation rate $\Gamma(T)$ we observed the drops floating at the liquid level and determined the times at which the different drops froze. The calculation of Γ was complicated by the fact that some drops left or entered the field of view of the microscope during the observation time. In addition, the number of drops changed because of coalescence, and some drops were still liquid at the end of the observation time. Under these conditions it is straightforward to show that the value of Γ is given by

$$\Gamma=n_d\Big/\sum_i V_i\tau_i , \tag{46}$$

where n_d is the total number of drops that nucleated, V_i is the volume of the ith drop, and τ_i is the time that it was under observation as liquid, whether it froze at the end of that time or simply moved out of the field of view. Results are shown in Fig. 7. Notice that these data are for $\Gamma(T)$ in the presence of a pressure P which also varies with temperature.

We have studied the statistics of the freezing process. At a temperature of 11 K we measured the lifetimes $\{\tau_i\}$ of $N_0=136$ drops with volumes $\{V_i\}$ between 5×10^{-7} and 2×10^{-6} cm^3. Figure 8 shows the number N of drops which have $V_i\tau_i$ greater than V_τ. If there is a constant probability Γ of nucleation per unit volume and unit time then we should have

$$N=N_0\exp(-\Gamma V\tau) . \tag{47}$$

The data are consistent with this law and a value of Γ of 4.1×10^4 cm^{-3} sec^{-1}. If we repeat this experiment with drops in a different size range, we again find an exponential law but the value of Γ is different even though the temperature is nominally the same. Thus, Fig. 8 also shows results with $5\times10^{-6}<V_i<2\times10^{-5}$ which give $\Gamma=8.5\times10^3$ cm^{-3} sec^{-1}. We always find in this way that the apparent value of Γ increases as the drop size decreases, i.e., small drops nucleate faster than they should.

We have considered several possible reasons for this effect. Since we can only measure drops which decay in a limited time range (roughly $\tau_{\min}=0.3$ sec to $\tau_{\max}=300$ sec), the measurement process inevitably introduces some bias into the data. Thus, regardless of the value of Γ, we will always find that for the drops which are seen to freeze, τ_i will be between $\tau_{\min}$ and $\tau_{\max}$. Hence, this causes the apparent value of Γ to vary with drop volume in the direction observed. However, a detailed simulation shows that this effect is too small to make Γ vary as rapidly as observed.

A second possibility is that the nucleation occurs only at the surface. This could occur if the surface energy between solid H_2 and helium gas is sufficiently low. Surface nucleation would make the apparent value of Γ (defined as rate per unit volume) vary as $V^{-1/3}$, which is

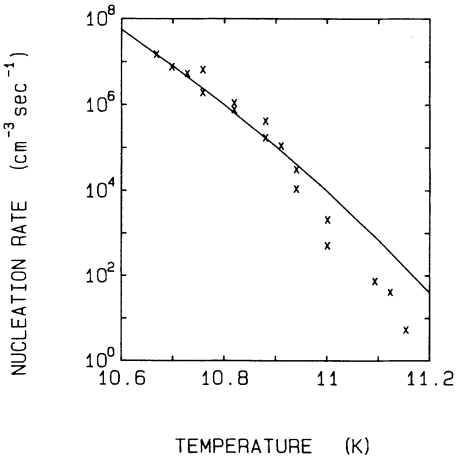

FIG. 7. Nucleation rate Γ as a function of temperature. The solid line is the result of a calculation of Γ using the value 0.874 cgs for the liquid-solid surface energy α_{LS}.

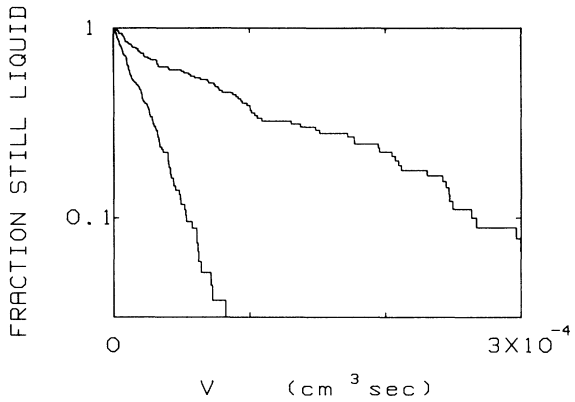

FIG. 8. Fraction of drops for which $V_i\tau_i$ is greater than $V\tau$ plotted as a function of $V\tau$. The upper data set is for drops with volumes $\{V_i\}$ between 5×10^{-6} and 2×5^{-5} cm^3, and the lower set with $\{V_i\}$ between 5×10^{-7} and 2×10^{-6} cm^3.

in the right direction. However, the variation observed experimentally is more rapid than $V^{-1/3}$. For example, with the change in volume of a factor of 10 between the two sets of drops included in Fig. 8, Γ changes by ~5, whereas $V^{-1/3}$ only changes by 2.2.

The most likely explanation of the effect of volume on nucleation rate is the cooling of the drops due to evaporation. In our cell it is not possible to keep the partial pressure of hydrogen equal to the saturated vapor pressure of the liquid at all points. We observe that usually liquid drops slowly evaporate. Consider what happens when a drop of liquid H_2 is placed in pure helium gas. After a short time a steady state will be set up in which H_2 diffuses away from the drop surface at a rate

$$\frac{dN}{dt}=4\pi R n_{\rm SVP} D \ , \tag{48}$$

where $n_{\rm SVP}$ is the number density of H_2 at the saturated vapor pressure, and D is the diffusion coefficient. The evaporation of the H_2 causes the drop to have a temperature different from the helium by an amount

$$\Delta T=\frac{-Dn_{\rm SVP}l}{\kappa_G} \ , \tag{49}$$

where l is the latent heat per molecule, and κ_G is the thermal conductivity of helium. We can estimate that at 11 K, $n_{\rm SVP}=2.3\times10^{19}$, $l=1.5\times10^{14}$ ergs, $\kappa_G=2900$ cgs. D has to be estimated from data at lower pressure; we use the value[31] 2×10^{-4} cm^2 sec^{-1}. This gives a ΔT of -0.024 K independent of the size of the drop. This calculation ignores the effect of gravity. The cold gas around the drop will sink, dragging the drop with it. This flow of the gas increases the cooling because the evaporation rate dN/dt will be increased when unsaturated helium is constantly being convected into the region near the surface of the drop. (In addition, the convection of the helium will cause the drop to have an equilibrium position slightly below the level where its density matches that of the helium fluid.) Thus, the drop will be colder than calculated using Table I. It seem likely, but it has not been proven, that the convection results in a larger $|\Delta T|$ for small drops than for big ones, and we believe that this is the reason for the apparent dependence of nucleation rate on size. To explain a factor of 10 variation in Γ one requires a temperature change of ~0.1 K, i.e., ~4 times the ΔT due to evaporation into helium at rest. An enhancement of ΔT of this amount due to convection is plausible.

In addition to this evaporation effect there is the ΔT due to flow induced by the surface tension discussed earlier. This flow lifts the drops to a warmer level, and also pulls down warmer helium into contact with the drop. This effect should make small drops warmer than large ones, and hence has a dependence on size opposite to that of evaporation. We have to assume that the evaporation effect dominates. To try to separate the two effects we looked at drops in a special cell in which we were able to produce a region with a very low vertical temperature gradient[32] (<0.5 K cm^{-1}). This should reduce the importance of flow induced by the surface tension relative to that produced by evaporation. We found that in this cell at 11 K the small drops floated at a lower height than larger ones, in support of this interpretation.

For these reasons there is an uncertainty in temperature of the drops, which at a nominal temperature 11 K might be as large as 0.2 K.[33] This error depends on the size of the drops and since different size drops have to be used at different temperatures (Γ varies by 10^6 over 0.6 K), there may be a substantial error in the results for the temperature dependence of Γ.

We have carried out several experiments to study the possible influence of impurities on the measured nucleation rate. The filtering system should remove impurities with high freezing temperatures.[33] It will not remove HD or D_2, however. In a separate experiment we added 1% D_2 to the H_2 and found that the nucleation rates were raised[34] by $\sim10^2$ at 11 K. Thus, one expects that the naturally occurring HD or D_2 impurities (0.015 at. % of D in H) will have a very small influence on the nucleation process. We also made a few measurements for normal hydrogen, n-H_2 (i.e., 75% ortho-H_2). In this case the nucleation rate was increased by $\sim10^3$. We think that this increase can be explained by the onset of rotational ordering in the solid phase. At high T both liquid and solid n-H_2 have an entropy of 0.75 ln3 arising from the degeneracy of the $L=1$ ortho molecules. (There is also a spin entropy which does not depend on temperatures, and can therefore be ignored.) As the temperature is lowered, quadrupolar interactions order the rotational moments in the solid and, to a much smaller extent, in the liquid. This decrease in the entropy and free energy of the solid relative to the liquid causes the triple point of n-H_2 to be at 13.96 K, compared to 13.81 K for p-H_2. From the measured quadrupolar specific heat[35] of solid n-H_2 we can estimate the quadrupolar contribution, $\delta F^Q_{\rm LS}$, to the difference in free energies of the liquid and solid at lower temperatures. At 11 K we find $\delta F^Q_{\rm LS}$ is 0.27 K, whereas our estimate[2] of $\delta F_{\rm LS}$ for p-H_2 was 2.59 K. This change in the free-energy difference results in a change in the nucleation

rate of $\sim 10^4$ at 11 K, in rough agreement with our measurements.

IV. DISCUSSION

Figure 7 includes the theoretical dependence of the rate for thermal nucleation[2] based on an assumed value of 0.874 cgs for the liquid-solid surface energy. This calculation includes corrections to allow for the applied pressure and the variation of this pressure with temperature. We have chosen α_{LS} to fit the data in the lower part of the temperature range where the effects of evaporation should be less important. As discussed above, the temperature dependence of Γ cannot be determined accurately experimentally, so the discrepancy between theory and experiment is not considered significant.

We can use the value of α_{LS} to estimate the nucleation rate in the absence of applied pressure. At a pressure of 15 bars, as we have in the present experiment, the density of the liquid is only 1.7% greater than at zero pressure. We therefore assume that α_{LS} still has the value of 0.874 at $P=0$. Results of the calculation of $\Gamma(T)$ are shown in Fig. 9 (curve A). The maximum nucleation rate Γ_{max} occurs at 7 K and has a value $\sim 10^{16}$ $\sec^{-1}\,\mathrm{cm}^{-3}$. This calculation assumes a temperature-independent value of α_{LS}. Even a small temperature dependence to α_{LS} causes a very large change in Γ_{max}. A model for the temperature dependence has been proposed by Woodruff,[36] who assumed that

$$\frac{d\alpha_{LS}}{dT}=\frac{d\alpha_{LG}}{dT}\frac{\alpha_{LS}}{\alpha_{LG}} . \tag{50}$$

The temperature dependence of α_{LG} in the range 14–20 K can be fitted by[37]

$$\alpha_{LG}=3.84-0.004\,63T^2 . \tag{51}$$

Then using (50) and $\alpha_{LS}=0.874$ at 10.7 K we obtain

$$\alpha_{LS}=1.014-0.001\,22T^2 . \tag{52}$$

The calculated value of $\Gamma(T)$ using Eq. (52) for α_{LS} is shown as curve B in Fig. 9. The value of Γ_{max} in this case is $\sim 10^{12}\ \sec^{-1}\,\mathrm{cm}^{-3}$.

Let τ_{max} be the time it takes to cool a drop of radius R through the temperature range near the maximum. To avoid nucleation we need

$$\tfrac{4}{3}\pi R^3\tau_{max}\Gamma_{max}<1 . \tag{53}$$

Thus, if curve B is correct we need $\tau_{max}<2\times10^{-3}$ sec for 10-μm-diam drops, and $\tau_{max}<2$ sec for 1 μm drops. A limit to the cooling rate of a drop is set by the thermal diffusivity of the liquid. The characteristic time τ_c for heat to be conducted out of a sphere whose surface is cooled is of the order of R^2/D_L, where D_L is the thermal diffusivity of the liquid. D_L is fairly slowly varying and at T_3 has the value $1.5\times10^{-3}\ \mathrm{cm}^2\sec^{-1}$. Thus, for 1- and 10-$\mu$m-diam drops τ_c is 1.7×10^{-6} and 1.7×10^{-4} sec, respectively. These times are therefore much shorter than needed.

There are two other interesting problems that may stand in the way of the production of superfluid H_2.

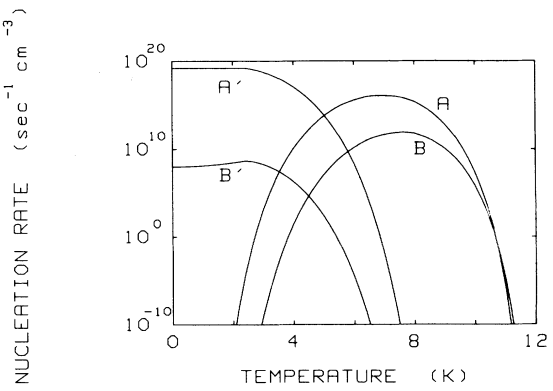

FIG. 9. Calculated nucleation rates. A and B are the rates for classical nucleation using a constant α_{LS} and allowing for some temperature dependence of α_{LS}, respectively, as discussed in the text. A' and B' are the corresponding rates for quantum tunneling through the barrier.

The first is the possibility that even if liquid H_2 does not freeze into a crystalline solid, a glass transition may occur. The various hydrodynamic effects we have observed are consistent with the assumption that the viscosity has a value not very different from that extrapolated from data above T_3. Thus, at least down to 10.6 K there is no sign of a rapidly increasing viscosity which might be expected if the system were approaching a glass transition.

The second problem is tunneling through the nucleation barrier, as distinct from thermal activation. Using the Lifshitz-Kagan theory[38] as evaluated in Ref. 2, we have calculated the nucleation rate Γ_Q via quantum tunneling for $\alpha_{LS}=0.874$ cgs, and for α_{LS} given by Eq. (50). The results are included in Fig. 9. If α_{LS} stays constant at 0.874, Γ_Q is $\sim 10^{19}\ \mathrm{cm}^{-3}\sec^{-1}$ at low T, and this would make a superfluid experiment very difficult, since even a drop of 0.1 μm diameter would have a lifetime of only 2×10^{-4} sec. With the temperature-dependent α_{LS}, Eq. (52), the value of Γ_Q is only $\sim 10^8$ $\mathrm{cm}^{-3}\sec^{-1}$, a value which would not create a problem working with drops of 1 μm size. Thus, the importance of Γ_Q is dependent on the small (and unknown) temperature dependence of α_{LS}. Note, however, that as discussed in Ref. 2 the Lifshitz-Kagan theory may substantially overestimate Γ_Q.

We have constructed an apparatus which can cool drops of diameter ~ 10 μm very rapidly and will report on these experiments separately.

ACKNOWLEDGMENTS

We thank G. S. Kanner and J. G. Cardon for help with the experiment, and R. S. Subramanian for discussions about the hydrodynamics. This work was supported in part by the National Science Foundation though Grants No. DMR-8501858 and No. DMR-8304224.

APPENDIX

To find the equation of state for fluid helium we have used the data of Hill and Lounasmaa.[39] We took their raw data points on $\rho=0.074\,10$, $0.077\,06$, and $0.081\,80$ g cm^{-3} for $9\leq T\leq 12.5$ K and fitted these points by the expression

$$P=A_1+A_2\rho'+A_3\rho'^2+A_4T'+A_5T'^2+A_6\rho'T' \quad \text{(A1)}$$

where $\rho'\equiv(\rho-\rho_0)/\rho_0$, $T'\equiv(T-T_0)/T_0$, and $\rho_0=0.080\,00$ g cm^{-3}, $T_0=10.8$ K. This gives (in bars)

$$A_1=14.948,\quad A_4=25.37\ ,$$

$$A_2=18.37,\quad A_5=-0.56\ ,$$

$$A_3=51.77,\quad A_6=38.15\ .$$

This fits each of the eight data points to better than $\pm 0.1\%$, which is less than the uncertainty in the data. The equation of state we need is slightly modified by the presence of a small concentration of H_2 in the ^{4}He. We have estimated this correction from the measured solubility[40] X_H of H_2 in ^{4}He. For a pressure of 13.8 bars the solubility can be fitted to the form

$$X_H=18\exp(-101/T)\ . \quad \text{(A2)}$$

At 10 K X_H is 7×10^{-4}, and at 12 K it is 4×10^{-3}. We corrected the density and the presence for the hydrogen fraction. For the pressure we simply assumed that the H_2 makes a contribution $n_{H_2}kT$, where n_{H_2} is the H_2 number density. This correction is only 0.2% at 12 K.

The density of liquid p-H_2 has been measured from 14 to 20 K by Scott and Brickwedde.[41] They fitted their data by

$$\rho_L(T)=2.016/(24.902-0.0888T+0.013\,104T^2)\ . \quad \text{(A3)}$$

We have simply extrapolated this into the region below T_3. Equation (A3) is strictly a fit at the saturated vapor pressure, but below T_3 this is essentially equivalent to the density for $P=0$. To obtain an equation of state for nonzero pressure, we have used the isothermal bulk modulus $B(T)$ given by McCarty *et al.*[3] We took their values for the range 14–20 K, and fitted the temperature dependence by

$$B(T)=A_0-A_2T^2\ . \quad \text{(A4)}$$

We then used this to extrapolate their data to the range below T_3. This correction to the density was made to first order in P, and was typically $\sim 1\%$. An additional correction has to be applied to allow for the solubility of the ^{4}He in the H_2. At 13.8 bars the solubility data[40] can be fitted to the form

$$X_{^4\mathrm{He}}=0.25\exp(-55/T)\ . \quad \text{(A5)}$$

Thus, at 11 K the ^{4}He concentration is 0.17%, and only a very rough correction is needed. To make this correction we assumed that the volume occupied by a ^{4}He atom in the liquid is the same as that of a H_2 molecule, and that the pressure is a function only at T and the total number density.

The final result for the pressure for neutral buoyancy is shown in Table I.

---

*Permanent address: Service de Physique du Solide et de Résonance Magnétique, Centre d'Etudes Nucléaire de Saclay, F-91191 Gif-sur-Yvette Cédex, France.

[1]A preliminary account of this work has been published: G. M. Seidel, H. J. Maris, F. I. B. Williams, and J. G. Cardon, Phys. Rev. Lett. **56**, 2380 (1986).

[2]H. J. Maris, G. M. Seidel, and T. E. Huber, J. Low Temp. Phys. **51**, 471 (1983).

[3]For a compilation of hydrogen properties, see R. S. McCarty, J. Hord, and H. M. Roder, *Selected Properties of Hydrogen (Engineering Design Data)*, Nat. Bur. Stand. Monograph No. 168 (U.S. GPO, Washington, D.C., 1981).

[4]There is also the possibility of quantum tunneling, as we discuss in Sec. IV.

[5]One does expect α_{LS} to depend somewhat on T; we discuss this later.

[6]See, for example, R. E. Apfel, J. Acoust. Soc. Am. **59**, 339 (1976).

[7]A. Ashkin and T. M. Dziedzic, Appl. Phys. Lett. **19**, 283 (1971).

[8]Grade HSC-197, from Airproducts, Inc., New Jersey.

[9]We could not resolve the details of this process.

[10]American Optical Company Model 580—Zoom.

[11]This was a conventional glass double Dewar.

[12]The nucleation occurs at an unknown time t_N somewhere between two consecutive frames. To prepare Fig. 3 we have had to estimate the value of t_N based on observations of the drop during the first few frames after nucleation.

[13]R. Clift, J. R. Grace, and M. E. Weber, *Bubbles, Drops, and Particles* (Academic, New York, 1978), Chap. 5.

[14]See G. S. Raithby and K. G. T. Hollands, Adv. Heat Transfer **11**, 280 (1975). This formula is for the steady-state rate of heat loss.

[15]This assumes that the fraction f of solid which is present immediately after nucleation is distributed uniformly throughout the drop.

[16]This calculation can also be used to derive the convective heat-loss term in Eq. (8) correct to within a numerical factor of order unity.

[17]We are taking the velocity gradient in the layer to the $2v/d$.

[18]Recall that when the drop nucleates it is almost neutrally buoyant. Thus, Eq. (17) makes the stronger statement that they will continue to go up, even when they have completely frozen provided that they are still hot.

[19]See, for example, E. M. Lifshitz and L. P. Pitaevskii, *Physical Kinetics* (Pergamon, Oxford, 1981), p. 55.

[20]They will occur because the temperature dependence of the thermal conductivity of the glass walls of the cell is different

from the temperature dependence of the conductivity of the helium gas. Thus, in the cell there will be horizontal temperature gradients which must lead to convection.

[21]There is, in fact, an apparent variation in height with distance from the axis (regardless of drop size) because of the variation of the refractive index of the helium with height. This causes an apparent distortion of the plane containing the drops.

[22]For a small flow the motion of the fluid will not disturb the temperature gradient.

[23]N. O. Young, J. S. Goldstein, and M. J. Block, J. Fluid Mech. **6**, 350 (1959).

[24]The effect of a finite Marangoni number on the thermocapillary migration velocity of a droplet in the absence of gravity has been calculated in R. S. Subramanian, Adv. Space Res. **3**, 145 (1983). This calculation cannot be applied directly to our experiment because the flow is modified by gravity, but it shows that the convection does give a significant correction.

[25]M. Meyappan and R. S. Subramanian, J. Colloid. Interface Sci. **97**, 291 (1984).

[26]D. M. Mattox, M. D. Smith, W. R. Wilcox, and R. S. Subramanian, J. Am. Ceram. Soc. **54**, 437 (1982).

[27]See, for example, P. D. Brazier-Smith, S. G. Jennings, and J. Latham, Proc. R. Soc. London, Ser. A **326**, 393 (1972); A. Podvysotsky and A. A. Shraiber, Int. J. Multiphase Flow **10**, 195 (1985).

[28]R. W. Park, Bull. Am. Meteoral. Soc. **51**, 578 (1970).

[29]This is true even when one allows for the difference in surface tension and density of water and hydrogen.

[30]H. Lamb, *Hydrodynamics* (Dover, New York, 1945). One has to extend Lamb's results slightly to derive Eqs. (43)–(45).

[31]E. A. Mason (private communication).

[32]This compares with the usual temperature gradient ~ 1.5 K cm^{-1}.

[33]In Ref. 1 we have described an experiment in which impurities were deliberately introduced.

[34]This increase is less than we reported earlier in Ref. 1.

[35]We used the data of R. W. Hill and B. W. A. Ricketson, Philos. Mag. **45**, 277 (1954).

[36]D. P. Woodruff, *The Liquid-Solid Interface* (Cambridge University Press, London, 1972), p. 30.

[37]V. N. Grigoriev and N. S. Rudenko, Zh. Eksp. Teor. Fiz. **47**, 92 (1964) [Sov. Phys.—JETP **20**, 63 (1965)]. They fitted their data to a linear temperature dependence. This implies a constant surface entropy. Equation (51) implies a surface entropy linear in T, which is plausible since the entropy of the liquid has this temperature-dependence and the entropy of the solid is small.

[38]I. M. Lifshitz and Y. Kagan, Zh. Eksp. Teor. Fiz. **62**, 385 (1972) [Sov. Phys.—JETP **35**, 206 (1972)].

[39]R. W. Hill and O. V. Lounasmaa, Philos. Trans. R. Soc. London **252**, 44 (1960).

[40]W. B. Street, R. E. Sonntag, and G. I. van Wylen, J. Chem. Phys. **40**, 1390 (1964).

[41]R. B. Scott and F. G. Brickwedde, J. Chem. Phys. **5**, 736 (1937).